Calibration and characterisation with a new laser-based magnetostriction measurement system

A. Rafferty *, S. Bakir, D. Brabazon, T. Prescott

School of Mechanical and Manufacturing Engineering, Dublin City University, Glasnevin, Dublin 9, Ireland

ABSTRACT

A laser-based magnet measurement system has been developed to measure the magnetostrictive strain of large cylindrical samples. The measurement system incorporates a solenoid capable of generating a maximum magnetic field intensity of 3000 Oe and a laser displacement sensor. For calibration and evaluation purposes, the positive magnetostrictions of two different types of giant magnetostrictive Tb–Dy–Fe-based materials were accessed with this system. A magnetostrictive strain of 622 ppm was obtained at 3000 Oe for $Tb_xDy_{1-x}Fe_{2-y}$, compared with 725 ppm for $Tb0._{27}Dy_{0.73}Fe_2$. A rod of sintered cobalt ferrite was also measured. This exhibited negative magnetostriction, with a maximum contraction of 260 ppm at 3000 Oe.

1. Introduction

Magnetostriction describes the effect that when a substance is exposed to a magnetic field, H, the dimensions of material change [1]. As depicted in Eq. (1), the fractional change in length A1/1 is a strain denoted by the symbol i,, in order to distinguish it from strain caused by an applied stress, e:

$$\lambda = \frac{\Delta l}{l}$$

The value of), measured at magnetic saturation is called the satura-tion magnetostriction, As. Most ferromagnetic materials exhibit some magnetostriction. If the magnetostriction is positive, the sam-ple elongates in the direction of the applied field irrespective of the direction of rotation of the magnetic moments and the thickness perpendicular to the applied field reduces such that the volume re-mains constant. If the magnetostriction is negative, the sample length decreases and the thickness increases [2].

One of the most significant developments in magnetostriction technology was the discovery of a new class of rare earth interme-tallic compounds, the RFe2 Laves phases, where R is a rare earth element such as terbium (Tb) or dysprosium (Dy) [3].

Among these materials, a terbium dysprosium iron alloy, often called Terfenol-D (Tb0.27Dy0.73Fe2) has attracted much interest because of its low magnetic anisotropy, combined with a positive saturation magne-tostriction (sat) of 1100 microstrain [3]. Terfenol-based cylinders are fabricated using a crystal growth manufacturing process [3]. Such magnetostrictive cylinders can be used in high strain and high force applications including vibra-tion, linear displacement, ultrasonic sensors, and actuators [4]. An-other recent research application of Terfenol-based materials has been as the emitter material in a sensor to measure very large cur-rents [5]. The estimates of the primary current come from a piezo-electric attached to the magnetostrictive material. In this work the authors used a TX-GMM cylinder (Tb„Dy_{1-x} Fe_2,) as the emitter component, but they highlight the difficulties which arise from the use of active materials which possess hysteretic behaviour or intrinsic non-linear behaviour. Satpathi et al. built an optical current transducer which contained an emitter of Terfenol-D, and a fibre Bragg grating that converted the magnetostrictive response into a wavelength modulated optical signal and transmitted it via an optical fibre for measurement [6]. Although successful to a point, problems were encountered due to the hysteretic nature of the Terfenol-D, which adversely affected the behaviour and performance of the system. For example, the phase shift between the ref-erence primary current and the output strain signal was not constant and shifted across the cycle, even under ideal operating conditions. The phase lags between the input and output were con-sidered too large to be explained by the intrinsic hysteretic effect of the Terfenol. A separate experiment revealed that that eddy cur-rents were contributing as much as 22° to the overall phase lag.

Terfenol-D is expensive, extremely brittle and the high content of rare earth metal makes the material extremely susceptible to corrosion. Terfenol-D also suffers from the problem of induced eddy currents, common to all metallic magnetic materials, which gives rise to ohmic losses and consequently decreases the performance (extension) of the magnetostrictive material [7]. The effect of eddy currents in Terfenol-D is a particularly severe because the material is very brittle and therefore difficult to laminate, as is done for example with transformer cores. Recently, this limitation has been addressed by the development of composite materials in which small particles of Terfenol-D are bonded with a nonconducting polymer binder [3]. However, despite some advantages, including easier machinability and moldability of specific sizes and shapes, magnetostrictive composites exhibit lower saturation magnetostriction than the monolithic material [8].

A solution to the problem of eddy currents is the use of a low electrical conductivity magnetostrictive material. One material which falls into this category is cobalt ferrite ceramic ($CoFe_2O_4$). McCallum et al. have developed cobalt ferrite and metal-bonded cobalt ferrite composites for potential use as sensors in lightweight power-steering technology [9]. Cobalt ferrite materials show a steep slope of magnetostriction at low applied fields which pro-vides a high sensitivity of extension to applied magnetic field. This extension is accentuated upon the application of a positive stress, a, on the sample in the direction of the applied field. The application of stress to a magnetised sample therefore gives high signal-to-noise ratios in sensor applications [10]. Materials used in this way make use of the Villari effect, which is the inverse of magnetostriction, i.e. a change in magnetisation due to applied stress. Their increased sensitivity, range and low electrical conductivity make materials based on this effect good candidates as new magnetomechanical sensor materials.

Magnetos triction can be measured by direct and indirect meth-ods. Examples of direct measurement methods include strain gauges, capacitance transducers, micrometer screw, or dilatometers [11]. Brizzolara and Colton described a novel device which uses a tunnelling tip as a position-sensitive detector and was noted as being capable of measuring displacements of 0.01 nm [12]. An extremely sensitive method for the measurement of small samples is the capacitance method, in which the deformation of the sample is measured as a change in the capacitance between two metal plates, one of which is fixed on the sample and the other of which is attached to the sample holder [13]. Sample deformation changes the capacitance between the plates which can be measured using a capacitance bridge. A difficulty of the capacitance method is the very delicate wiring required to reduce floating capacitances. An-other drawback is that an electrode must be mounted on the sur-face of the sample prior to measurement which can cause stressing of small samples.

Although not often presented in recent literature, optical measurement methods are amongst the oldest indirect magnetostriction measurement methods. A major advantage of optical methods is that no contact is required between the probe and the sample. Hirano et al. used a Keyence laser displacement meter to measure the magnetostriction of silicon steel sheet samples [14]. Phway et al. describe magnetostriction measurement of silicon steel sheets for a range of frequencies, using a single point laser Doppler vibrometer for fields up to 414 Oe [15]. Lorenz et al. constructed a device incorporating a laser beam and four-quadrant photodiode for high temperature magnetostriction measurements of sheet samples up to a maximum field of 370 Oe [16]. This paper presents testing with a recently commissioned low-cost laser-based magnetostriction measurement device, for measuring large-scale cylinders up to a maximum magnetic field intensity of 3000 Oe.

2. Magnetostriction measurement system design

2.1. System components

Fig. 1 shows the main elements of the system and their arrange-ment. A precision dual power supply (Zantrex XFR 300-9, Thurlby Thandar Instruments, UK) was used to supply a steady DC current to the solenoid coil. A laser measurement system (Model RD-50RW, Keyence Ltd., UK) was employed to measure the sample dis-placement to an accuracy of ±1 vim. The copper wire was wound around a wooden solenoid former of 26 mm inner diameter and 137 mm length. Wooden discs were attached to the ends of the former as retaining flanges. The wood offered no resistance or distortion to the magnetic field generated by the solenoid.

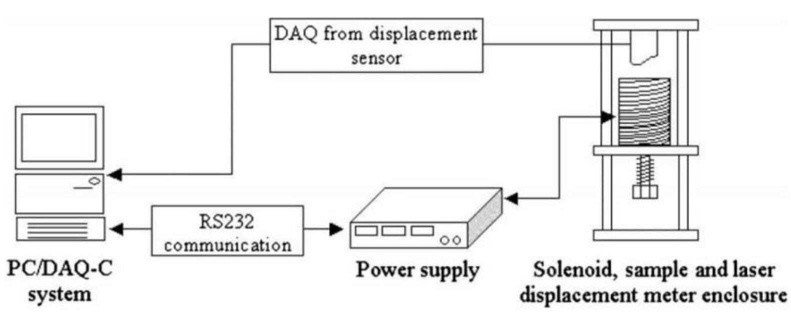

Fig. 1. Schematic of the magnetostriction measurement system indicating the PC/DAQ-C system, power supply, solenoid and the laser displacement meter enclosure.

2.2. Displacement measurement

Test specimens were inserted into nylon bushings which were custom-made to fit tightly inside the wooden former. The bushings was also shaped to tightly grip the bottom 10 mm of the cylinders tested such that the base of the sample did not move when the solenoid was energised. A solid nylon insert pressed into the bottom of the former provided a regular sample height. The supporting assembly was made from an epoxy resin with a low thermal expansion coefficient to minimise interference with the magnetic field during testing. The laser head was mounted on a micrometer stage which could be raised or lowered into the correct range for specimen displacement measurement. Each sample was measured five times and an average taken.

The displacement data was recorded with a high precision 24 bit data acquisition card (NI PC-451 and LabVIEW Version 8.2, National Instruments). A LabVIEW programme was written to allow simultaneous incremental increases in current from 0 to 6 A (in 0.2 A increments) and recording of the sample displacement. Sample exposure to the magnetic field was kept below 2 s and times between magnetising were set to 2 s (or greater for high-er currents) in order to prevent the heating of the solenoid coil and hence sample.

2.3. Solenoid design

A copper wire solenoid consisting of 5555 turns was constructed. Table 1 shows the specifications of the wire used.

Table 1
Specifications of the enamelled copper wire used to make the solenoid

Resistivity (Ω m)	SWG	Diameter (mm)	Diameter incl insulation (mm)	Density (kg/m^3)	SHC (J/kg °C)
1.724×10^{-8}	22	0.71	0.776	9920	387

In order to reduce the difficulties associated with manual winding, seven individual coils were connected in series. The completed solenoid comprised 34 layers, 5555 turns, and was 76 mm in diameter. Theoretical magnetic field strengths generated by the solenoid were calculated based on the well-known formula [17]:

$$H=\frac{NI}{\sqrt{4r^2 \ + l^2}}$$

Where N is the number of loops or turns of windings, I is the current flow through the coil, r is the effective radius of the coil, and 1 is the length of the coil.

The calculated magnetic field strengths from a current of 6 A for the seven individual coils are shown in Table 2. The average measured completed solenoid resistance was 42.42 S-2 which agreed well with theoretical calculation.

Table 2
Predicted cumulative magnetic field strengths for the coils

Coil	Cumulative windings	Cumulative magnetic field strength (kA/m)	Cumulative magnetic field strength (Oe)
1	1175	49.38	620.81
2	2171	90.41	1136.61
3	2988	123.43	1551.69
4	3661	150.15	1887.95
5	4315	175.68	2208.95
6	4947	199.9	2513.39
7	5555	222.74	2800.59

2.4. Magnetic flux density of solenoid

A hand-held Hall effect gaussmeter (Model 5080, Sypris Solutions Ltd., USA) was used to measure the magnetic flux density at the centre of the solenoid. As shown in Fig. 2, the magnetic flux density, B, varied linearly with respect to current and reached a maximum value of 2992 G at 6 A. The ratio of magnetic flux to magnetic field is defined as permeability, pt. In air relative permeability, per, is equal to one, where the magnitudes of magnetic field (Oe) and magnetic flux (G) are numerically equal. To avoid confusion, from now on the term magnetic field strength will be used in this paper as opposed to magnetic flux, as the magnetic field in this work was generated in air.

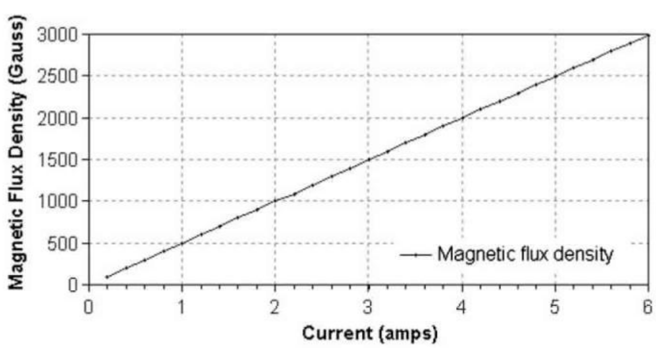

Fig. 2. Variation of solenoid magnetic flux density with respect to current.

2.5. Cobalt ferrite (CoFe204) rod fabrication

$CoFe_20_4$ powder was attrition milled (Molinex Type PE075, Net-zsch Ltd., Germany) to a particle size of 5 um. Using a mixer and hotplate, 3 wt% PVA and 3 wt% glycerine were dissolved in distilled water. The $CoFe_2O_4$ powder was blended into this binder solution and mixed thoroughly. The powder was dried and packed into a cylindrical-shape rubber bag (Trexler Rubber Ltd., Ohio, USA). The rubber bag was encased in a cardboard tube to prevent bulging of the bag during filling. Tapping and plunging was employed to compact the powder inside the bag. A vacuum pump was used to remove the air from the bag, thus providing an initial pre-pressing. These measures ensured that an almost perfect cylinder was devel-oped during wet-bag isostatic pressing (Stansted Fluid Power Ltd., UK). The rod was sintered using a 2-step sintering process devel-oped previously [18].

Crucially, the quality of the cylinder produced was such that post-sinter machining was unnecessary. Previous experience had shown that pure cobalt ferrite rods are prone to fracture during machining. While the bulk of the rod was not tampered with, the ends were ground flat. After grinding, the rod measured 100 mm in length and 20 mm in diameter.

Additions of small quantities of silver and nickel to cobalt ferrite is one way to improve the mechanical strength, yielding rods capable of withstanding post-sinter machining. However, such metallic elements were avoided in this work as they would invariably increase the materials electrical conductivity and susceptibility to eddy currents.

3. Results and discussion

Two samples of Tb-Dy-Fe-based giant magnetostrictive cylindrical rods (100 mm long and 20 mm in diameter) were sourced commercially; Terfenol-D ($Tb_{0.27}Dy_{0.73}Fe_2$) from Etrema Ltd. (USA), and TX-GMM ($Tb_xDy_{1-x}Fe_{2-y}$) from Tianxing Rare Earth Functional Materials Ltd. (TXRE Ltd., China). Certificates of authen-ticity were supplied to verify the compositions of both of the sam-ples. Since composition determines magnetostrictive response, any departure from the optimum Tb:Dy ratio or Tb/Dy:Fe ratio will af-fect performance. Both samples had good tolerances (length 100 mm ± 0.1 mm and diameter 20 mm ± 0.1 mm), and good per-pendicularity between the end surfaces. From visual inspection, the surface of the $Tb_{0.27}Dy_{0.73}Fe_2$ rod was extremely homogeneous relative to the $Tb_xDy_{1-x}Fe_{2-1}$,, which exhibited minor defects (see Fig. 3). Non-uniform metallurgical structure and defects, including poor grain size, grain misorientation, pores or cracks can often result in variations in performance of samples. Surface defects can also signal premature sample failure, particularly in the case of materials which are subject to cyclical magnetostrictive displacements during their working life.

Fig. 3. Picture of surface detail of the cobalt ferrite ($CoFe_2O_4$), Terfenol-D ($Tb_{0.27}Dy_{0.73}Fe_2$) and TX-GMM ($Tb_xDy_{1-x}Fe_{2-y}$) samples.

The three samples under investigation in this work were tested using the developed magnetostrictive measurement system. The data recorded was smoother for the $Tb_{0.27}Dy_{0,73}Fe_2$; the standard deviation calculated over the five samples was less than the Tb_xDy_{1-x} Fe_{2-y} (±3.5 for $Tb_{0.27}Dy_{0.73}Fe_2$ vs. ±4.2 for Tb_xDy_{1-x} Fe $_{2-y}$). The results are shown in Fig. 4.

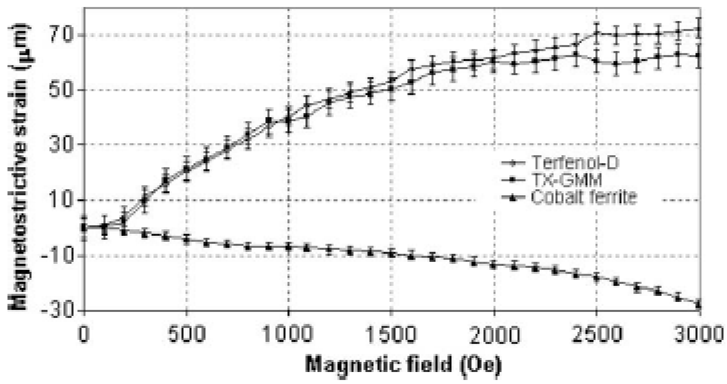

Fig. 4. Magnetostrictive strain response of Terfenol-D ($Tb_{0.27}Dy_{0.73}Fe_2$), TX-GMM ($Tb_xDy_{1-x}Fe_{2-y}$) and cobalt ferrite ($CoFe_2O_4$).

As can be seen from Fig. 4, the $Tb_{0.27}Dy_{0.73}Fe_2$ and Tb_xDy_{1-x} Fe_{2-y} samples demonstrated quite similar expansion behaviour up to 2500 Oe, above which they began to deviate. Both of the samples exhibited linear behaviour in the range 400-800 Oe. Beyond 800 Oe, the behaviour turned non-linear and approached saturation magnetostriction at >2500 Oe. The linear region is the optimal working range, and is preferred for converting the magnetic into mechanical energy because of the minimisation of losses. The mag-netostrictive coefficient d33 is the slope of the strain vs. magnetic field characteristic: di,./dh. For effective and efficient operation, d33 needs to be as high as possible. For Terfenol-D the value of the magnetostrictive coefficient d33 is in the range 5-70 x 10^{-9} A^{-1} m [19].

The negative magnetostriction (contraction) recorded from the CoFe204 rod is also plotted in Fig. 4. The absolute magnetostrictive strain response of the CoFe204 is approximately half the strain exhibited by the Tb-Dy-Fe-based materials. A distinct linear mag-netisation region is observed up to approximately 600 Oe. In this low field regime a magnetostrictive coefficient d33 of 1.4 x 10-9 A -1 m was recorded. Another distinct quasi-linear region is then ob-served up to 2000 Oe. After this point the curve begins to lose its linearity. The point of saturation magnetostriction is not observed. Saturation magnetostriction of CoFe204 is not expected to occur until approximately 5000 Oe.

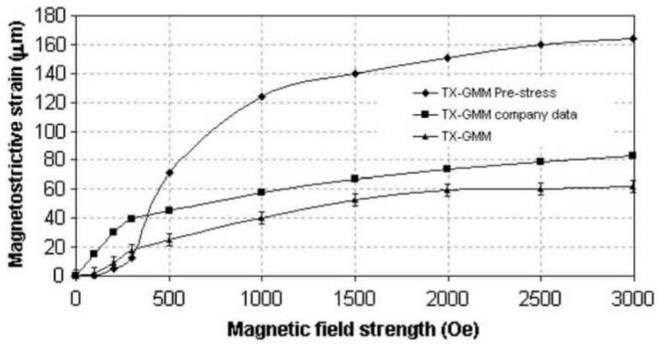

Fig. 5. Magnetostrictive strain of TX-GMM ($Tb_xDy_{1-x}Fe_{2-y}$) with and without pre-stressing.

In Fig. 5, the bottom two curves show the experimentally mea-sured data in this work for Tb_xDy_{1-x} Fe_{2-y} ,alongside the data which was supplied by TXRE Ltd. The shape of these curves are in good agreement although a difference in magnetostrictive strain of approximately 20 p.m between the TX-GMM manufacturers data and that recorded in this work does exist. No data was available to attach error bars to the data supplied by TXRE Ltd. It should be pointed out that no stress was applied during the tests carried out in this experimental work. The application of a stress tends to change the shape of the magnetostriction curve quite dramatically. This effect is illustrated by the top curve in Fig. 5 which is data for a sample measured under a pre-stress of 10 MPa.

The pre-stressed sample exhibits some variation in the mea-sured magnetostriction. The shape of the curve is classical; com-prising two distinct magnetisation regions. In the low field region (up to 300 Oe) domain wall motion occurs. The region from 300 to 750 Oe is termed the "burst" region, where the strain-field slope is maximum. This region arises due to reorientation of mag-netic moments (produced at the atomic level by electron spins) from an "easy" crystallographic axis perpendicular to the applied field to one more closely aligned with the applied field. Easy axes correspond to orientations for the magnetic moment vectors that satisfy local crystallographic energy minimisation states in the magnetostrictive material as the applied stress and magnetic field vary.

4. Discussion

According to Chen et al., $CoFe_2O_4$ exhibits a better strain deriv-ative or slope of magnetostriction (62/6H), at low applied fields compared to $Tb_{0.27}Dy_{0.73}Fe_2$, which contributes to a high sensitiv-ity to magnetic field, hence giving high signal-to-noise ratio and excellent linearity of response [10]. $CoFe_2O_4$ is an oxide ceramic, making it less susceptible to eddy currents, and to non-linear behavioural response. Chen et al. used strain gauges to measure saturation magneto-striction of silver and nickel-containing cobalt ferrite (2/98 vol% $Ag_{0.97}$ $Ni_{0.03}$, + CoO • Fe_2O_3), cylinders (15 mm long and 5 mm in diameter) [10]. A maximum value of —225 ppm was measured. The magnetostriction then decreased with increasing field, as the magnetisation of the particles or grains were rotated away from the easy directions. Bozorth et al. measured a saturation magneto-striction of -250 ppm for single crystal cobalt ferrite of composition $Co_{1.1}Fe_{1.9}O_4$ [20]. Recently, Lo et al. claimed improvements in magnetostriction of $CoFe_2O_4$ as a result of magnetic annealing, which induced uniaxial anisotropy and affected domain configuration and magnetisation processes [21]. By annealing $CoFe_2O_4$ at 300 °C in air for 36 h under a DC field of 318 kA/m (4 kOe), the maximum magnetostriction increased in magnitude from —200 ppm to —252 ppm. Furthermore, the magnetostrictive coeffi-cient d33 increased from 1.5 x 10-9 A-' m to 3.9 x 10-9 A-1 m. Lo et al. stress that the magnetomechanical properties of magnetically annealed samples may degrade over time or after operation at ele-vated temperatures, and further work is required to examine the longer term stability of the induced anisotropy of the magnetically annealed samples. Tb-Dy-Fe-based samples subjected to a pre-stress can exhibit more than a twofold increase in magnetostrictive strain. $Tb_{0.27}Dy_{0.73}Fe_2$ is very brittle in tension (tensile strength is typically 28 MPa) but has a reasonable compressive strength (700 MPa). Small pre-stresses result in increased saturation mag-netisation, but if the pre-stress is too high the pre-stress energy overpowers the elastic energy produced by the material and the magnetostriction decreases. According to Ono et al., the magneto-striction of $(Tb\text{-}Dy)Fe_2$ Laves phase compounds is strongly dependent on pre-stress [22]. Optimum magnetostrictions were re-corded in the range 10-20 MPa, but these showed a dramatic decline with increasing pre-stress in the range 20-40 MPa.

5. Conclusions

A low-cost laser-based magnetostriction measurement system has been developed to measure the magnetostrictive strain of large cylindrical samples. With this system, magnetic field strengths up to 3000 Oe were generated. Magnetostriction measurements were conducted on giant magnetostrictive Tb-Dy-Fe based cylindrical rods which were sourced from two different commercial suppliers for analysis and system calibration. Both exhibited positive, non-linear magnetostrictive strain response, with values in good agree-ment with those in the literature. A magnetostrictive strain of 622 ppm was obtained at 3000 Oe for Tb_xD_{y-1},Fe_2,, compared with 725 for $Tb_{0.27}$ $Dy_{0.73}$,Fe_2. A rod of sintered $CoFe_20_4$ exhibited negative magnetostriction, with two distinct regions of linearity and a maximum contraction of 260 ppm at 3000 Oe.

Acknowledgements

This work was supported by the European Commission through the IELAS project (Contract Number G5RD-CT-2001-0054) under the Competitive and Sustainable Growth Research Programme. This support is gratefully acknowledged.

References

[1] Cullity BD. Introduction to magnetic materials. USA: Addison-Wesley; 1972, ISBN 0201012189, p. 248.

[2] Dapino MJ, Calkins FT, Flatau AB. On identification and analysis of fundamental issues in Terfenol-D transducer modeling. Proc SPIE Smart Struct Mater 1998;3329:185-97.

[3] Piercy AR. The changing shape of magnetostriction. Phys Edu 1997;32:160-3.

[4] Cullity BD. Introduction to magnetic materials. USA: Addison-Wesley; 1972, ISBN 0201012189, p. 279-82.
[5] Lopez-Garcia 0, Carnicero A, Ruiz R, Talavera J, Mateo C. Development of a current sensor based on active materials for high-voltage transmission systems. Smart Mater Struct 2006;15:563-70.
[6] Satpathi D, Moore J, Ennis MG. Design of a Terfenol-D based fiber-optic current transducer. IEEE Sens J 2005;5:1057-65.
[7] Engdahl G, editor. Handbook of giant magnetostrictive materials. San Diego, USA: Academic Press; 2000, ISBN 012238640X, p. 158.
[8] McKnight GP, Carman GP. Large magnetostriction on Terfenol-D particulate composites with preferred [1 1 2] orientation. Proc SPIE 2001;4333:178-83.
[9] McCallum RW, Snyder JE, Dennis KW, Schwichtenberg CR, Jiles DC. US Patent No. 6,352,649; 2002.
[10] Chen Y, Snyder JE, Schwichtenberg CR, Dennis KW, McCallum RW, Jiles DC. Metal-bonded Co-Ferrite composites for magnetostrictive torque sensor. Appl IEEE Trans Mag 1999;35:3652-4.
[11] Gr6ssinger R, Sassik H, Holzer D, Pillmayr N, Accurate measurement of the magnetostriction of soft magnetic materials, 1&2-dimensional magnetic measurement and testing. Paper 1-5; 2000. p. 35.
[12] Brizzolara RA, Colton RJ. Magnetostriction measurements using a tunneling-tip strain detector. J Magn Magn Mater 1990;88:343-50.
['13] Samata H, Nagata Y, Uchida T, Abe S. New optical technique for bulk magnetostriction measurement. J Magn Magn Mater 2000;212:355-60.
[14] Hirano M, Ishihara Y, Harada K, Todaka T. A study on measurement of magnetostriction of silicon steel sheet by laser displacement meter. J Magn Magn Mater 2003;43:254-5.
[15] Phway TPP, Moses AJ, Jiles DC. Frequency dependence of magnetostriction for magnetic actuators. J Electr Eng 2004;55:7-10.
[16] Lorenz BE, Graham Jr CD. Apparatus for high temperature magnetostriction measurement of bulk samples. Rev Sci Instrum 2004;75:2770-2.
[17] Kraus JD. Electromagnetics. New York: McGraw-Hill; 1991, ISBN 0-07-035621-1
[18] Rafferty A, Prescott T, Brabazon D. Sintering behaviour of cobalt ferrite ceramic. Cers Int 2008;1:15-21.
[19] Janocha H, editor. Adaptronics and smart structures: basics, materials, design and applications. Berlin: Springer-Verlag; 1999, ISBN 3540614842, p. 124-43.
[20] Bozorth RM, Tilden EF, Williams AJ. Anisotropy and magnetostriction of some ferrites. Phys Rev 1955;99:1788-98.
[21] Lo CCH, Ring AP, Snyder JE, Jiles DC. Improvement of magnetomechancial properties of cobalt ferrite by magnetic annealing. IEEE Trans Mag 2005;41:3676-8.
[22] Ono H, Shimada M, Toma H. Magnetostrictive properties of a new type of Tb-Dy-Fe-Zn Laves phase compound. J Appl Phys 2000;88:7213-6.